NREL National Renewable Energy Laboratory
A national laboratory of the U.S. Department of Energy
Office of Energy Efficiency & Renewable Energy
Innovation for Our Energy Future

Novel High Efficiency Photovoltaic Devices Based on the III-N Material System

Final Technical Report
7 December 2005 – 29 August 2008

C. Honsberg, W.A. Doolittle, and I. Ferguson
University of Delaware
Newark, Delaware

Subcontract Report
NREL/SR-520-44186
October 2008

NREL is operated for DOE by the Alliance for Sustainable Energy, LLC Contract No. DE-AC36-08-GO28308

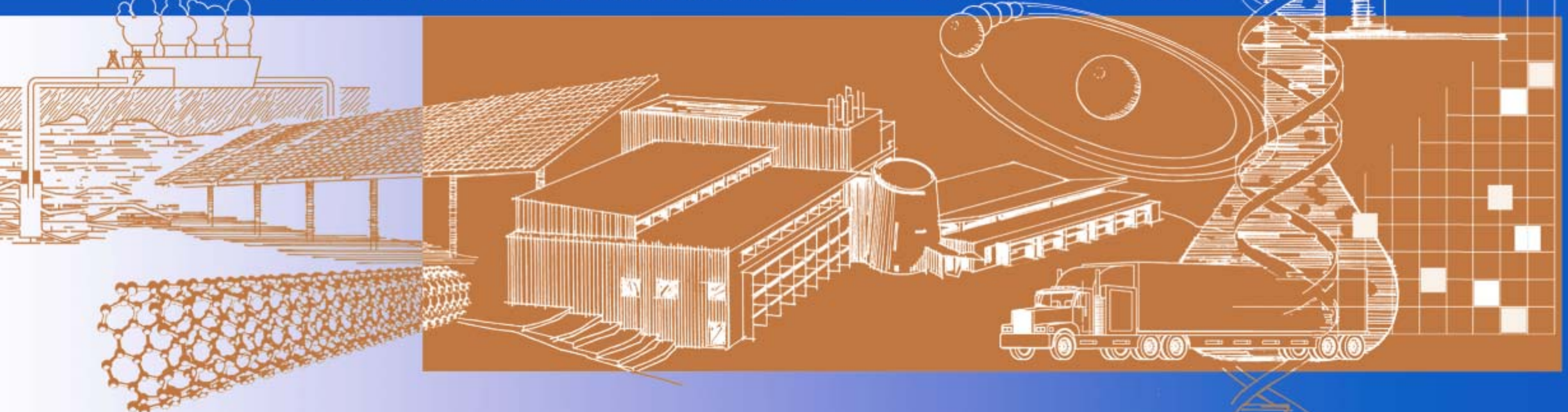

Novel High Efficiency Photovoltaic Devices Based on the III-N Material System

Final Technical Report
7 December 2005 – 29 August 2008

C. Honsberg, W.A. Doolittle, and I. Ferguson
University of Delaware
Newark, Delaware

NREL Technical Monitor: L. Greene and M. Symko-Davies
Prepared under Subcontract No. XEJ-6-55157-01

Subcontract Report
NREL/SR-520-44186
October 2008

National Renewable Energy Laboratory
1617 Cole Boulevard, Golden, Colorado 80401-3393
303-275-3000 • www.nrel.gov

NREL is a national laboratory of the U.S. Department of Energy
Office of Energy Efficiency and Renewable Energy
Operated by the Alliance for Sustainable Energy, LLC

Contract No. DE-AC36-08-GO28308

Available electronically at http://www.osti.gov/bridge

Available for a processing fee to U.S. Department of Energy
and its contractors, in paper, from:
U.S. Department of Energy
Office of Scientific and Technical Information
P.O. Box 62
Oak Ridge, TN 37831-0062
phone: 865.576.8401
fax: 865.576.5728
email: mailto:reports@adonis.osti.gov

Available for sale to the public, in paper, from:
U.S. Department of Commerce
National Technical Information Service
5285 Port Royal Road
Springfield, VA 22161
phone: 800.553.6847
fax: 703.605.6900
email: orders@ntis.fedworld.gov
online ordering: http://www.ntis.gov/ordering.htm

Printed on paper containing at least 50% wastepaper, including 20% postconsumer waste

Introduction

The initial motivation for the project laid in the then-newly discovered band gap of InN, re-measured at ~0.7 eV rather than the previous 1.9 eV [1-3]. This makes InGaN a potential material for solar cell with the possibility to absorb 99% of the solar irradiance. The advantages of the InGaN material system are the wide range of direct band gap, high absorption coefficient, a low effective mass (high mobility), and strong polarization effects [4-6]. However, the challenges include material quality, defect density, doping, substrates and growth issues. The current project led to the understanding of the above challenges; in particular the material quality in terms of phase separation was studied and suppressed. The polarization property was modeled and solar cell design was developed with these new models.

The following section describes the issue of phase separation and its suppression. Then a brief description of polarization and its modeling is presented. The effect of phase separation and polarization on device operation follows. The next section presents the solar cell design and results achieved.

Phase Separation and Its Suppression

There exists a solid phase miscibility gap in the InGaN alloy due to the large difference in the lattice constants between GaN and InN, which is also the probable cause of multiple phases and consequent multi-peak luminescence observed in the material [7,8]. The equilibrium solubility of InN in the bulk GaN is approximately 6% at typical growth temperatures used in MOCVD. However, the situation in thin InGaN films epitaxially deposited on GaN virtual substrates is significantly different. Theoretical calculations [9] based on a valence-force-field (VFF) model [7, 10] predict that phase separation in InGaN strongly depends not only on the temperature and In composition, but also on the strain state of the InGaN films. Thus, one or more indium-rich phases come into existence in the InGaN alloy layers during growth in an attempt to reach thermodynamic equilibrium during growth as shown in Figure 1.

Phase separation is usually identified as secondary peaks in addition to the primary peak corresponding to the bulk material during photoluminescence and, while higher degrees of phase separation are also identified via X-ray diffraction (XRD), shown in Figure 2.

In addition to acting as a recombination channel, it can be correlated from fabricated quantum-well solar cells that the lower-band gap phase separated material will also tend to pin down the open-circuit voltage (V_{OC}) of the solar cell.

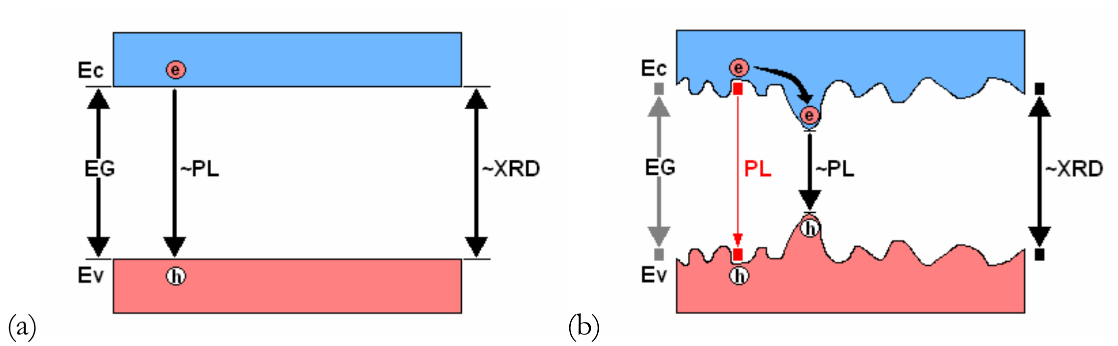

Figure 1: Schematic comparison of band structures of (a) an ideal material, and (b) a phase separated material.

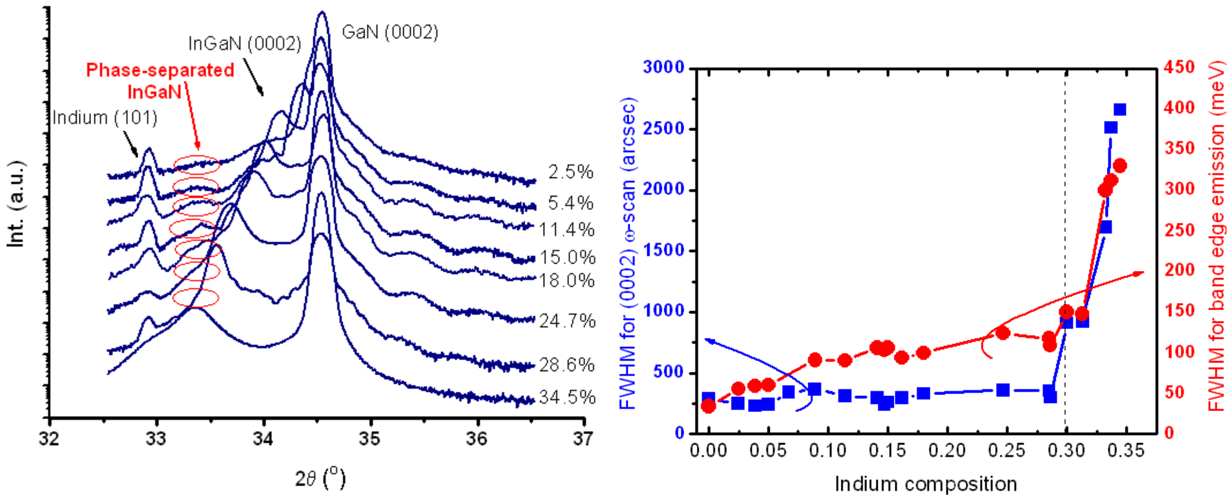

Figure 2: Summary of (a) Photoluminescence (PL) (b) PL and X-ray diffraction data for InGaN grown by MOCVD with indium composition ranging from 0 to 35%.

To minimize the effect of phase separation and increase the material quality of the grown layers, the effect of TMIn flow, temperature, growth pressure, growth rate and TEGa flow were examined and optimized. The effect of TMIn flow is shown in Figure 3. Increasing the flow rate suppresses the secondary peak in PL signals, indicating that phase separation is suppressed.

The effect of growth temperature is shown in Figure 5. As the growth temperature is decreased, the surface morphology becomes rough and the growth mode changes from step growth to nucleation of discrete islands. However, the growth temperature, in conjunction with the TEGa flow rates determines the growth rate, which also influences phase separation and the indium composition. As the TEGa flow rate increases, the FWHM of XRD increases, indicating poorer material quality.

The final critical parameter in controlling phase separation is the thickness of the layer. The effect of thickness is shown in Figure 4. Figure 4 shows, the appearance of a secondary phase of lower band gap InGaN with In ≈ 10% for thickness of 100nm. Further optimization allows minimization of the phase separation for layers as thick as 200 nm.

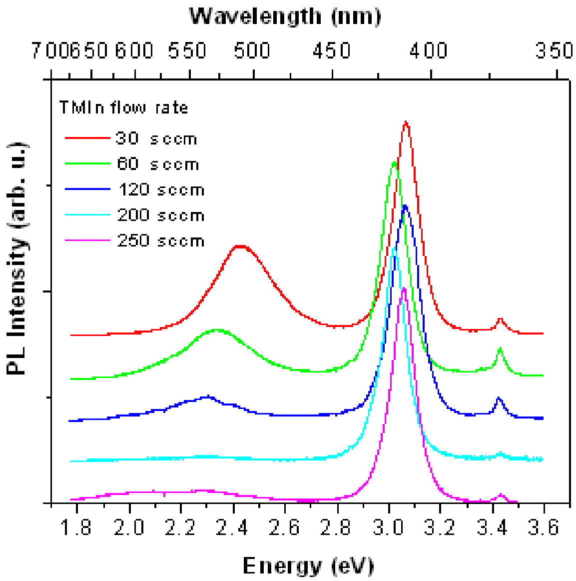

Figure 3: PL data summary of InGaN growth with variable TMIn flow rate.

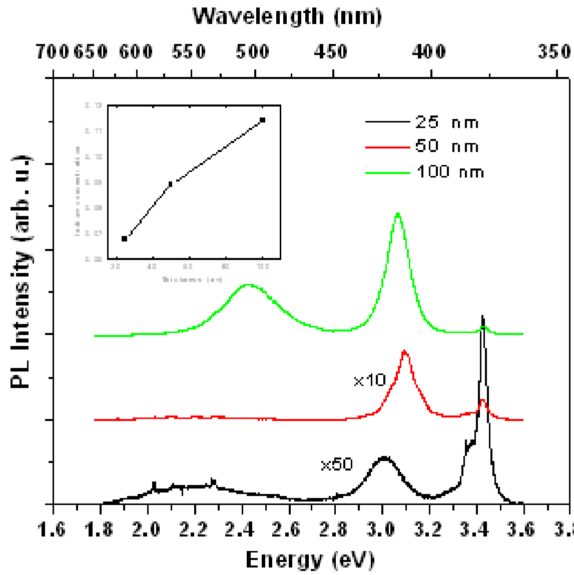

Figure 4: Photoluminescence data indicating increasing emission from phase separated InGaN with increasing thickness.

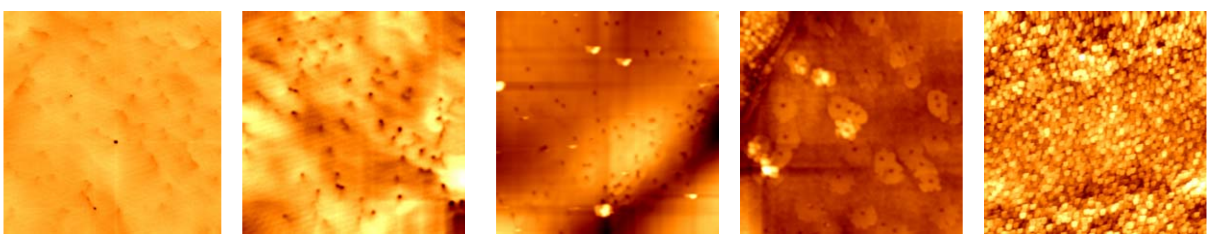

Figure 5: Effect of growth temperature on surface morphology, showing change of growth mode from step-like growth to nucleation of discrete islands.

Polarization Modeling

One of the unique characteristics about the wurtzite III-nitrides is its polarization effects. The net polarization, Spontaneous polarization ($\vec{P}_{sp}$) + Piezoelectric polarization ($\vec{P}_{pz}$), and consequent internal electric fields have been shown to be detrimental to the performance of optoelectronic devices [11-13]. Polarization discontinuities lead to potential barriers, band bending that can have undesired consequences on the device; electric fields with values as high as 1 MV/cm have been reported [14, 15]. Polarization, however, can be utilized constructively by accommodating in the solar cell design to improve its performance. Thus, it becomes vital to successfully model this effect and incorporate it during device design.

Polarization is present in the III-nitrides as a consequence of the non-centrosymmetry of the wurtzite structure and the large ionicity of the covalent metal-nitrogen bonds. Spontaneous polarization ($\vec{P}_{sp}$) exists due to the non-centrosymmetry of the crystal, where the crystal behaves like an electric dipole. In the III-nitrides, the direction of spontaneous polarization is from the N-atom to the closest metal atom, i.e. along the ±c direction, which is also the typical MOCVD or MBE growth direction. Hence, in Ga-face GaN, spontaneous polarization is opposite to the [0001] direction, i.e. in the downward direction pointing towards the substrate as shown in Figure 6(a).

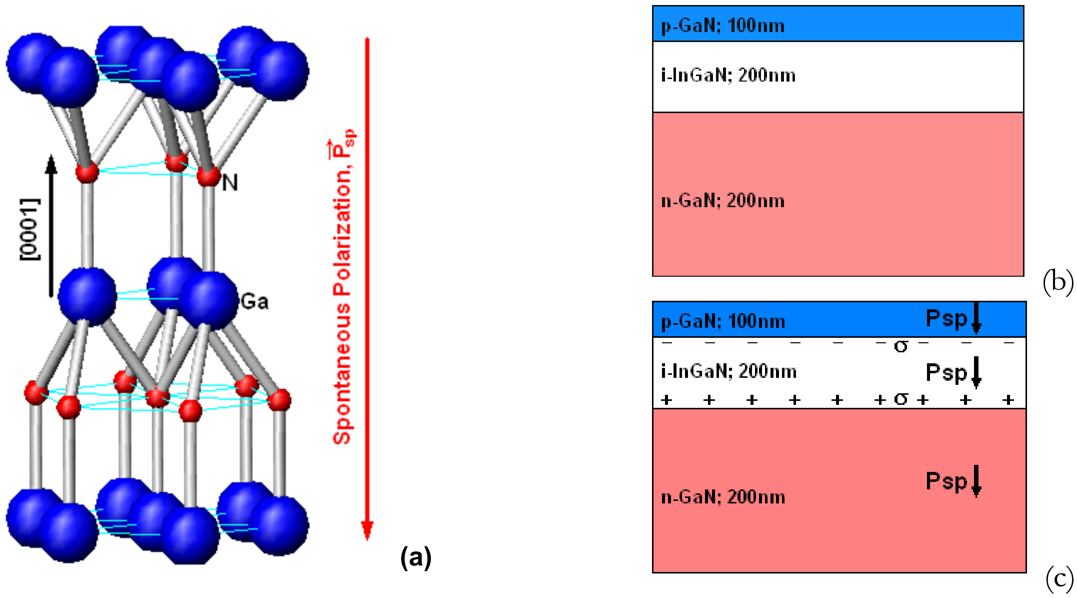

Figure 6 (a) Direction of spontaneous polarization jn Ga-face GaN and GaN/InGaN p-i-n test structure (b) without and (c) with spontaneous polarization effects

Spontaneous polarization in ternary compounds can be calculated by interpolating the binary compounds using a bowing factor 'b' as shown in Equation 1.

$$P_{sp}^{ABN}(x) = P_{sp}^{AN}(x) + P_{sp}^{BN}(1-x) + bx(1-x) \qquad \text{[Units: C/m}^2\text{]} \qquad (1)$$

The direction of piezoelectric polarization is dependent on the polarity of the material as well as on the strain, shown in Figure 6(b). Spontaneous and piezoelectric polarizations are parallel and add to each other when planar strain (perpendicular to c-axis) is tensile and are anti-parallel when planar strain is compressive.

The polarization-induced charge density with a gradient of polarization in space given by:

$$\sigma_P = -\nabla P \qquad \text{[Units: C/m}^2\text{]} \qquad (2)$$

The polarization-induced charge density or electric field is used as the starting point for the modified PC1D solving routine at a given hetero-interface. If the charge density at a hetero-interface is positive, it will tend to accumulate a 2-Dimensional Electron Gas (2DEG); similarly, a negative hetero-interface charge density will tend to form a 2-Dimensional Hole Gas (2DHG).

The modified PC1D, incorporates polarization, is used in the design of InGaN solar cells. The design of pn-junction solar cells starts with a p-i-n structure and evolves to the current status of utilizing n-GaN capping layer. Alongside the design and fabrication of pn-junction solar cells alternative approaches in designing solar cells are considered. The pn-junctions and alternative approaches are presented in the next section.

Device Design and Results

Two approaches have been attempted in the design of InGaN solar cells, pn-junction solar cells and Schottky-barrier solar cells. This section presents the evolution of InGaN pn-junction solar cell designs fabricated and tested is summarized in Figure 7, followed by results of Schottky-barrier solar cells.

The solar cells are designed, grown by MOCVD/MBE, fabricated, characterized and analyzed before designing the next generation of devices. The p-i-n device structure (Figure 7(a)) is taken as the starting point to design subsequent InGaN solar cells due to a detailed understanding obtained from preliminary experiments. The indium composition in the test devices is fixed at 12% (E_g – 2.9 eV) to ensure successful p-type and n-type doping. Here, the p- and n-GaN regions are fixed at 100 nm and 500 nm thicknesses, respectively and doped at maximum concentrations without reaching a level of degeneracy. The thickness of the i-region is fixed at 200 nm.

As the i-InGaN region adds to the series resistance of the solar cell, this region is replaced by a p-n InGaN junction in second-generation solar cells as shown in Figure 7(b). In this case, the additional electric field generated by the InGaN p-n junction enhances the QE of the solar cell. Moreover, the p-GaN layer not only acts as a window layer for the underlying InGaN p-n junction, but the GaN junctions also induce front and back surface fields for this device. The thicknesses of p- and n-InGaN are set to 50 nm and 150 nm, respectively to maintain a net InGaN thickness of 200 nm.

The I-V curves for the second-generation InGaN devices show a substantial improvement in short-circuit current of the solar cell compared to the first-generation devices as shown in Figure 8(a) and (b). The increase in short-circuit current is supported by the increase in internal quantum efficiency of the second generation devices up to 50% as seen in Figure 9. However, there is a decrease in the open-circuit voltage due to reduction in quasi-fermi level energy difference caused by additional doping in the InGaN junctions and/or formation of phase-separated defects. The third-generation InGaN devices are designed to minimize the voltage loss caused by the p-GaN window layer due to its high resistivity. Hence, the thickness of the p-GaN window layer is reduced from 100 nm to 10 m as shown in Figure 7(c). However, the 50 nm p-InGaN layer is not thick enough to provide charge to the depletion region, which results into an incomplete junction formation. Hence, these solar cells measure very low open-circuit voltages and quantum efficiencies.

The fourth-generation devices are designed to enhance the window layer by replacing the 10 nm p-GaN with n-GaN. The strained window layer forms a 2DEG at the n-GaN/p-InGaN interface, as explained in previous section, improving the lateral conduction in the material, while the n-GaN window enhances tunneling to reduce the top contact resistance of the device. However, these devices also fail to provide substantial open-circuit voltage and quantum efficiency due to incomplete charge provision by the thin p-junctions.

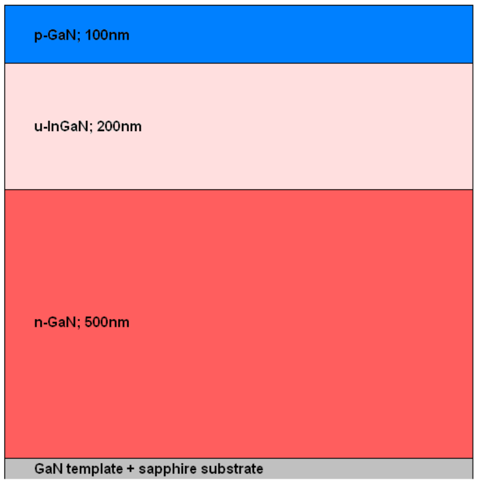

(a) Gen 1: p-i-n structure.

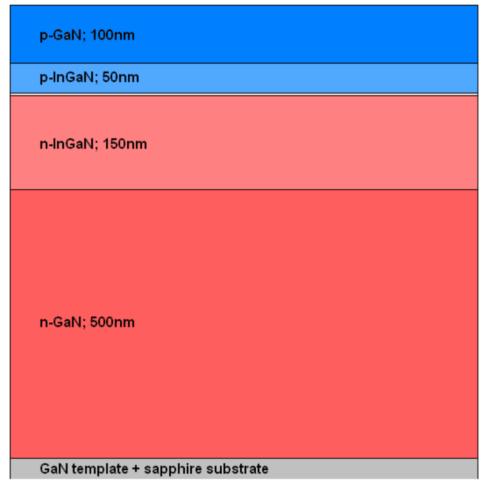

(b) Gen 2: i-InGaN replaced by p-n InGaN.

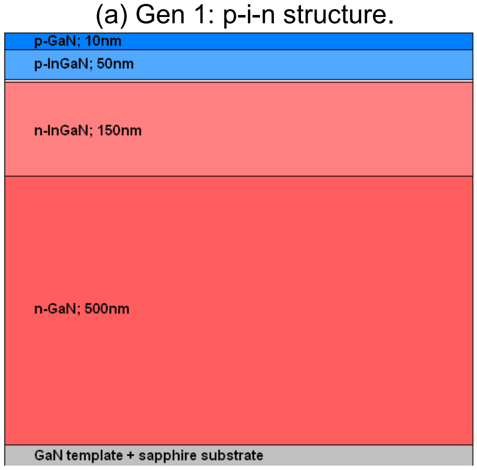

(c) Gen 3: Thickness of p-GaN reduced.

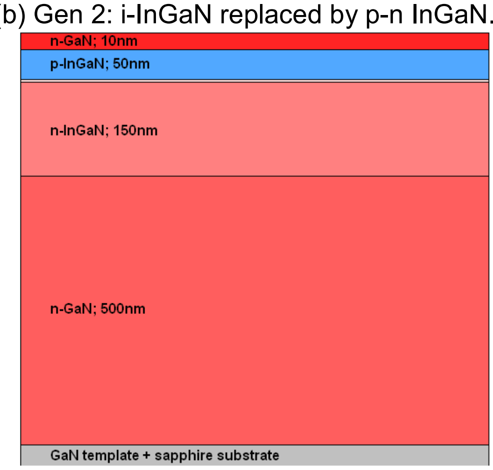

(d) Gen 4: p-GaN cap replaced by n-GaN.

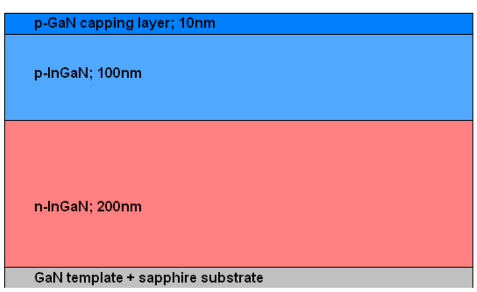

(e) Gen 5: Thickness of InGaN increased.

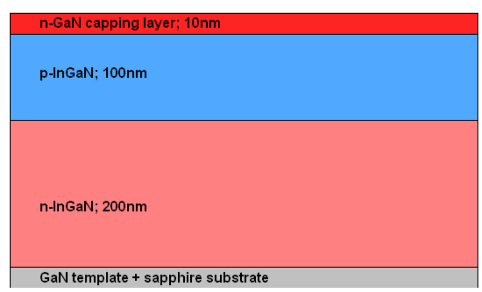

(f) Gen 6: Thickness of InGaN increased.

Figure 7: Generations of InGaN solar cell evolution.

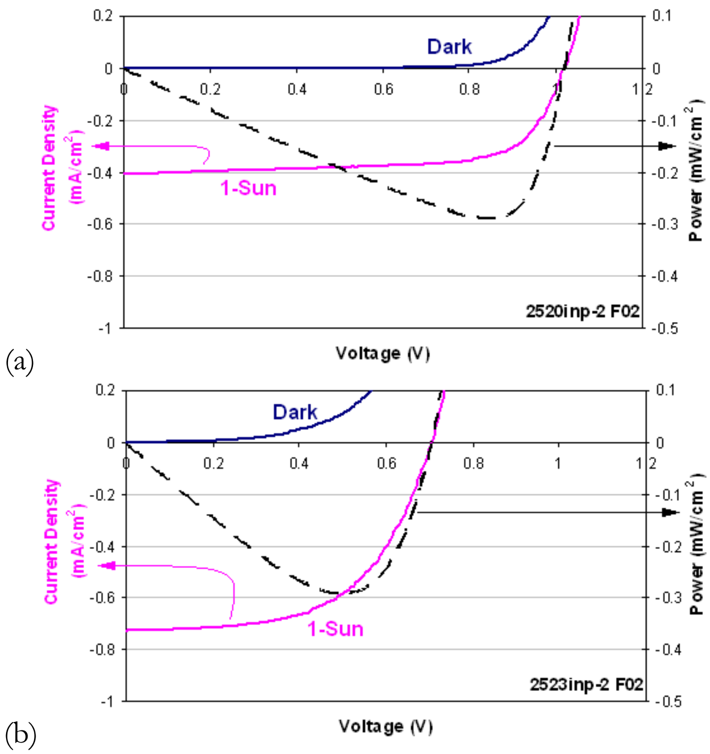

Figure 8: Sample I-V characteristics of (a) first-generation, and (b) second generation test solar cells.

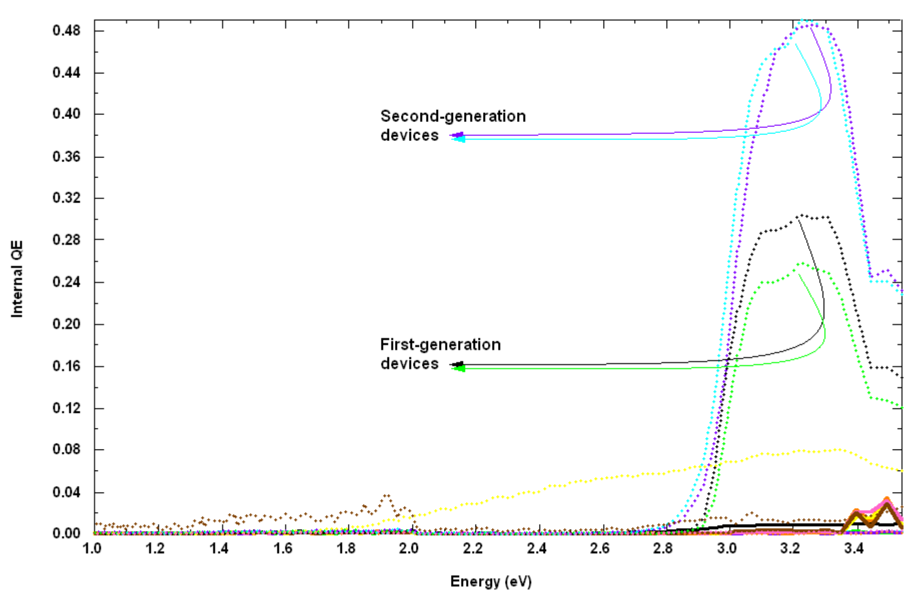

Figure 9: Internal quantum efficiency comparison of first and second-generation test solar cells.

The next generation solar cells are designed to overcome the limitations caused by the thin p-type InGaN junctions. Here, the thickness of InGaN p-n junction is increased to 300 nm, where the thickness of p- and n- InGaN are designed at 100 nm and 200 nm, respectively. The fifth and sixth-generation solar cells employ a 10 nm thick p- and n-GaN window layer, respectively. These devices yield a substantially higher performance compared to the fourth and fifth- generation devices. Highest open-circuit voltages are obtained from the sixth-generation solar cells, which employ a thin n-GaN tunneling window layer as shown in Figure 10.

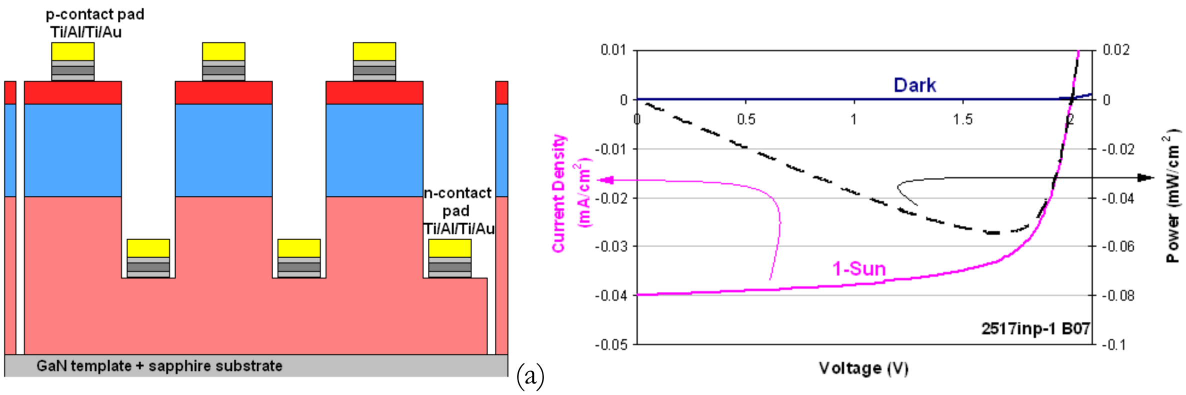

Figure 10: Sixth-generation (a) test solar cells structure (b) IV photo response.

The pn-junction InGaN solar cells have a good response but the understanding of the electrical and optical issues originating in each layer are better studied with Schottky-barrier devices. The Schottky device structures play an important role in understanding the electrical properties of the material along with being good alternative approaches for making solar cells. Two types of Schottky-barrier solar cells can be formed (a) Metal-Semiconductor (b) Metal-Insulator-Semiconductor. Each of these is presented below.

The difference between an Ohmic contact and Schottky contact is the difference in the work function between metal and semiconductor. In the present work a study of metal-InGaN is being studied. Figure 11 pictorially demonstrates the formation of Ohmic and Schottky junction.

Initial experiments on *p*-GaN were conducted with Ti/Au as the Schottky metal contact. The metal contacts were annealed in the temperature range of 550 ^{o}C and 700 ^{o}C. Below 550 ^{o}C no Schottky diodes were formed. At annealing temperatures greater than 650^{o}C the metal transformed into small clusters on the surface. Forming gas was used for gas flow, and no significant effect of gas flow rate was observed. The initial results are shown in Figure 12(a) for a Ti/Au metal contact to *p*-GaN annealed at 650^{o}C for 2 min in forming gas, highlighting the photovoltaic effect.

The Schottky-barrier heights are calculated based on Richardson plots Figure 12(b). The barrier height of the device is calculated using the following formula [16]:

$$\phi_B = \frac{V_1}{n} - \frac{k}{q}\frac{d[\ln(I/T^2)]}{d(1/T)},$$ where V_1 is a reference voltage, and n is the ideality factor.

The Schottky-barrier height is calculated to be 0.48 eV.

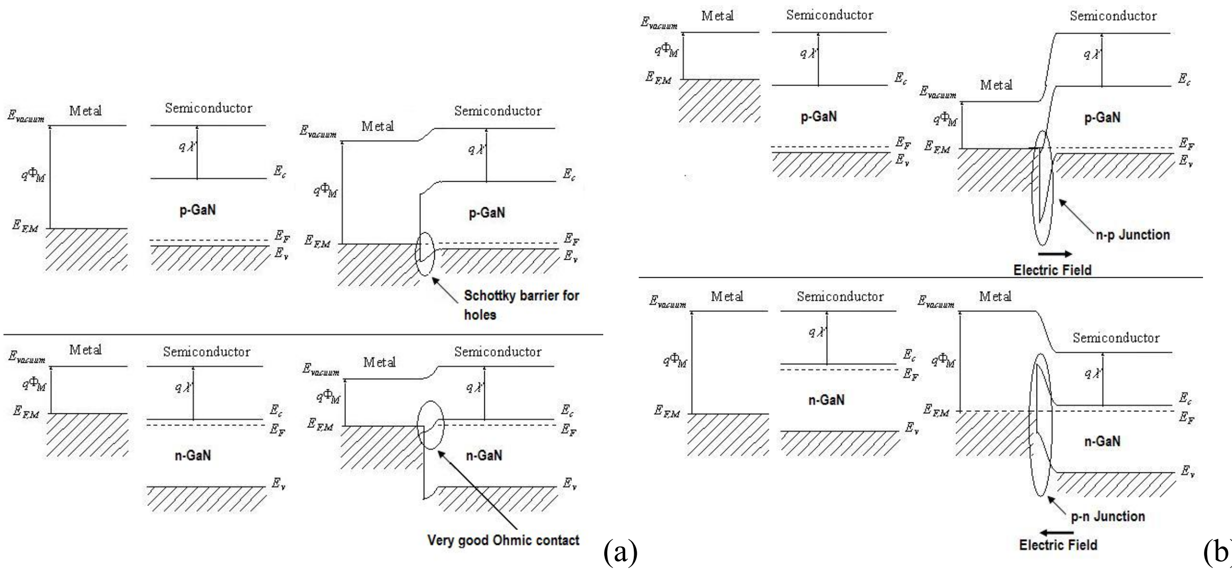

Figure 11: Metal-Semiconductor junction formation

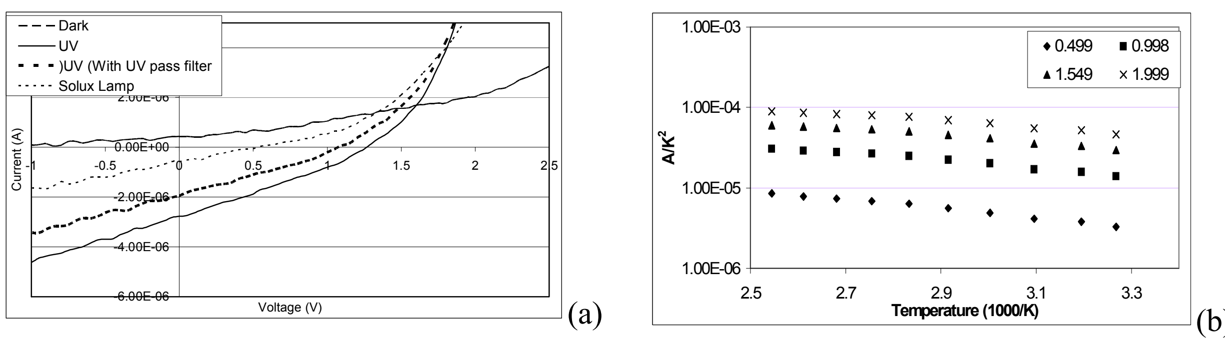

Figure 12: (a) IV results of Ti/Au metal-*p*-GaN Schottky junction (b) Richardson Plot

Conclusions

The current work researched into understanding InGaN as the potential material for photovoltaics. Phase separation was identified as a key loss mechanism. Phase separated material (a lower band gap) controls the open circuit voltage, while the non-phase separated material (higher band gap) controls the absorption. Phase separation in InGaN layers was controlled via optimization of growth conditions and device thickness.

InGaN solar cells with Voc ≈ Eg – 0.4 V and using 2.5 eV band gap have been demonstrated. This is the first report of (a) a InGaN solar cell with such a low band gap and (b) an open circuit voltage with approximately 0.4 V of the band gap, for any material composition in the InGaN material system. The realization of an open circuit voltage close to its practical limit for a new material system in such a short time frame is a major accomplishment. Internal quantum efficiency > 60% for near band gap light in GaN solar cells have been demonstrated. The ability to make photovoltaic devices without requiring a pn junction by using Schottky/MIS approaches has been demonstrated. These are the first reports of Schottky/MIS solar cells.

Modeling of polarization effects in InGaN solar cells has been implemented in PC1D. This is the first photovoltaic modeling to include peizo-electric and polarization effects in a solar cell model. Device design rules for InGaN solar cells, including the impact of p-i-n structures, the impact of polarization and piezoelectric properties of InGaN have been set forth.

In addition to material quality and growth, modeling and fundamental device design issues, fabrication and processing approaches have also been investigates. Of particular importance is the demonstration of ohmic contacts to InGaN solar cells using metal contacts and tunneling contacts have been demonstrated. Further, a standard processing sequence has been developed for the fabrication of InGaN solar cells.

Overall, the research shows that InGaN material system can be used to realize high efficiency solar cells, making contributions to growth, modeling, understanding of loss mechanisms, and process optimization.

REFERENCES:

1] V. Yu. Davydov, A. A. Klochikhin, R. P. Seisyan, V. V. Emtsev, S. V. Ivanov, F. Bechstedt, J. Furthmuller, H. Harima, A. V. Mudryi, J. Aderhold, O. Semchinova, and J. Graul, "Absorption and Emission of Hexagonal InN. Evidence of Narrow Fundamental Band Gap," Phys. Stat. Sol. B, vol. 229, 3, p. R1-R3, 2002.

2] T. Matsuoka, H. Okamoto, M. Nakao, H. Harima, and E. Kurimoto, "Optical Bandgap Energy of Wurtzite InN", Appl. Phys. Lett., 81, 7, p. 1246-1248, 2002.

3] J. Wu et al., "Temperature Dependence of the Fundamental Band Gap of InN", J. Appl. Phys., vol. 94, 7, p. 4457-4460, 2003.

4] F. Bernardini, and V. Fiorentini, "Nonlinear Macroscopic Polarization in III-V Nitride Alloys", Phys. Rev. B, 64, 8 (2001), p. 085207/1.

5] V. Fiorentini and F. Bernardini, "Spontaneous versus Piezoelectric Polarization in III-V Nitrides: Conceptual Aspects and Practical Consequences", Phys. Stat. Sol. B, 216 (1999), p. 391.

6] Y. Nanishi, Y. Saito and T. Yamaguchi, "R-F Molecular Beam Epitaxy Growth and Properties of InN and Related Alloys", Jpn. J. Appl. Phys., vol. 42, 5A, p. 2549-2559, 2003.

7] I. Ho, and G. B. Stringfellow, "Solid phase Immiscibility in GaInN," Appl. Phys. Lett., vol. 69, p. 2701, 1996.

8] S. Chichibu, T. Azuhata, T. Sota, and S. Nakamura, "Luminescence from Localized States in InGaN Epilayers," Appl. Phys. Lett., vol. 70, p. 2822, 1997.

9] V. A. Elyukhin and S. A. Nikishin, "Internal Strain Energy of AX3B1-X3N Ternary Solid Solutions of Cubic Modification," Semicond. Sci. Technol., vol. 11, p. 917-920, 1996.

10] I. H. Ho and G. B. Stringfellow, "Incomplete Solubility in Nitride Alloys," Mater. Res. Soc. Symp. Proc., vol. 449, p. 871-880, 1997.

11] P. Lefebvre, A. Morel, M. Gallart, T. Taliercio, J. Allègre, B. Gil, H. Mathieu, B. Damilano, N. Grandjean, and J. Massies, "High internal electric field in a graded-width InGaN/GaN quantum well: Accurate determination by time-resolved photoluminescence spectroscopy," Appl. Phys. Lett., vol. 78, p. 1252, 2001.

12] R. Langer, J. Simon, V. Ortiz, N. T. Pelekanos, A. Barski, R. André, and M. Godlewski, "Giant electric fields in unstrained GaN single quantum well," Appl. Phys. Lett., vol. 74, p. 3827, 1999.

13] F. Bernardini and V. Fiorentini, "Polarization fields in nitride nanostructures: 10 points to think about," App. Surface Science, vol. 166, p. 23, 2000.

14] J. C. Freeman, "Basic equations for the modeling of Gallium Nitride (GaN) High Electron Mobility Transistors (HEMT)," NASA/TM – 2003-211983.

15] O. Ambacher, J. Smart, J. R. Shealy, N. G. Weimann, K. Chu, M. Murphy,W. J. Schaff, L. F. Eastman, R. Dimitrov, L. Wittmer, M. Stutzmann, W.Rieger, and J. Hilsnbeck, "Two-dimensional electron gases induced by spontaneous and piezoelectric polarization charges in N- and Ga-face AlGaN/GaN heterostructures," J. Appl. Phys. 85 (1999), p. 3222.

16] Schroder, D. K. (1990). Semiconductor material and device characterization, Wiley

PUBLICATIONS:

[1] Christiana Honsberg, Omkar Jani, Alan Doolittle, Elaissa Trybus, Gon Namkoong Ian Ferguson, David Nicole, Adam Payne. “InGaN – A new solar cell material,” *19th European Photovoltaic Science and Energy Conference, Paris*, (2004). **Invited Oral Presentation**.

[2] Elaissa Trybus, Gon Namkoong, Walter Henderson, W. Alan Doolittle, Rong Liu, Jin Mei, Fernando Ponce, Maurice Cheung, Fei Chen, Madalina Furis, Alexander Cartwright. “Growth of InN on Ge substrate by molecular beam epitaxy”, *Journal of Crystal Growth* 279, 311–315, 2005.

[3] Omkar Jani, Christiana Honsberg, Ali Asghar, David Nicol, Ian Ferguson, Alan Doolittle, Sarah Kurtz, “Characterization and analysis of InGaN photovoltaic devices, *Conference Record of the Thirty-First IEEE Photovoltaic Specialist Conference (IEEE Cat. No. 05CH37608)*, Orlando, 2005, p 37-42. **Invited oral presentation**.

[4] Omkar Jani, Christiana Honsberg, Yong Huang, June-O Song, Ian Ferguson, Gon Namkoong, Elaissa Trybus, Alan Doolittle, Sarah Kurtz, “ Design, Growth, fabrication and characterization of high-band gap InGaN/GaN solar cells, *4th World Conference of Photovoltaic Energy Conversion*, May 2006. **Oral presentation**.

[5] Elaissa Trybus, Gon Namkoong, Walter Henderson, Shawn Burnham, W. Alan Doolittle, Maurice Cheung, Alexander Cartwright, “InN: A material with photovoltaic promise and challenges,” *Journal of Crystal Growth* 288 (2006) 218–224.

[6] M Mehta, O Jani, C Honsberg, B Jampana, I Ferguson, A Doolittle, “Modifying PC1D to model spontaneous and Piezo-electric polarization in III-V nitride solar cells,” *Proceedings of the 22nd European Photovoltaic Solar Energy Conference, Milan Italy*, (2007).

[7] Omkar Jani, Hongbo Yu, Elaissa Trybus, Balakrishnam Jampana, Ian Ferguson, Alan Doolittle, Christiana Honsberg. Effect of phase separation on performance of III-V nitride solar cells, *Proceedings of the 22nd European Photovoltaic Solar Energy Conference, Milan Italy*, (2007). **Oral presentation**.

[8] Nikolai Faleev, Christiana Honsberg, Omkar Jani, Ian Ferguson, “Crystalline perfection of GaN and AlN epitaxial layers and the main features of structural transformation of crystalline defects”, *Journal of Crystal Growth*, 300, 246–250, 2007.

[9] Omkar Jani, Ian Ferguson, Christiana Honsberg, Sarah Kurtz, “ Design and characterization of GaN/InGaN solar cells,” *Applied Physics Letters* 91, 132117, 2007.

[10] Yong Huang, Omkar Jani, Eun Hyun Park, and Ian Ferguson. “Influence of Growth Conditions on Phase Separation of InGaN Bulk Material Grown by MOCVD”, *Mater. Res. Soc. Symp. Proc. Vol. 955*, 2007.

[11] E. Trybus, O. Jani, S. Burnham, J. Bai, D. S. Citrin, I. Ferguson, W. A. Doolittle, C. Honsberg and M. Steiner, "Characteristics of InGaN Designed for Photovoltaic Applications", 7th International Conference of Nitride Semiconductors (ICNS-7), Las Vegas, NV, USA, September 16-21, 2007. **Oral Presentation**

[12] Yong Huang, Omkar Jani, Eun Hyun Park, and Ian Ferguson, “Influence of Growth Conditions on Phase Separation of InGaN Bulk Material Grown by MOCVD”, *Mater. Res. Soc. Symp. Proc.* Vol. 955 2007.

[13] Balakrishnam R Jampana, Omkar K Jani, Hongbo Yu, Ian Ferguson, Brian E McCandless, Steven S Hegedus, Robert L Opila, Christiana B Honsberg, “Nitride based Schottky-barrier photovoltaic devices,” *Proceedings of the Material Research Society Symposium*, 2007.

[14] Nikolai Faleev, Balakrishnam Jampana, Anup Pancholi, Omkar Jani, Hongbo Yu, Ian Ferguson, Valeria Stoleru, Robert Opila, and Christiana Honsberg. “High quality InGaN for photovoltaic applications: type and spatial distribution of crystalline defects and “phase” separation,” *Proceedings of the 33rd IEEE Photovoltaic Specialists Conference*, San Diego, May 2008. **Oral Presentation**.

[15] Omkar Jani, Balakrishnam Jampana, Mohit Mehta, Hongbo Yu, Ian Ferguson, Robert Opila, Christiana Honsberg. “Optimization of GaN window layer for InGaN solar cells using polarization effect,” *Proceedings of the 33rd IEEE Photovoltaic Specialists Conference*, San Diego, May 2008.

[16] E. Trybus, O. Jani, S. Burnham, I. Ferguson C. Honsberg, M. Steiner, and W. A. Doolittle. “Characteristics of InGaN designed for photovoltaic applications,” *phys. stat. sol. (c)* 5, no. 6, 1843–1845, 2008.

THESIS:

Omkar Jani, Development Of Wide-Band Gap InGaN Solar Cells For High-Efficiency Photovoltaics, PhD Thesis, Georgia Institute of Technology, 2008.

REPORT DOCUMENTATION PAGE

Form Approved
OMB No. 0704-0188

1. REPORT DATE *(DD-MM-YYYY)*
October 2008

2. REPORT TYPE
Subcontract Report

3. DATES COVERED *(From - To)*
7 December 2005 - 29 August 2008

4. TITLE AND SUBTITLE
Novel High Efficiency Photovoltaic Devices Based on the III-N Material System, Final Technical Report, 7 December 2005 - 29 August 2008

5a. CONTRACT NUMBER
DE-AC36-08GO28308

5b. GRANT NUMBER

5c. PROGRAM ELEMENT NUMBER

6. AUTHOR(S)
C. Honsberg, W.A. Doolittle, and I. Ferguson

5d. PROJECT NUMBER
NREL/SR-520-44186

5e. TASK NUMBER
PVA72401

5f. WORK UNIT NUMBER

7. PERFORMING ORGANIZATION NAME(S) AND ADDRESS(ES)
University of Delaware
201 Evans Hall
Newark, DE 19716

8. PERFORMING ORGANIZATION REPORT NUMBER
XEJ-6-55157-01

9. SPONSORING/MONITORING AGENCY NAME(S) AND ADDRESS(ES)
National Renewable Energy Laboratory
1617 Cole Blvd.
Golden, CO 80401-3393

10. SPONSOR/MONITOR'S ACRONYM(S)
NREL

11. SPONSORING/MONITORING AGENCY REPORT NUMBER
NREL/SR-520-44186

12. DISTRIBUTION AVAILABILITY STATEMENT
National Technical Information Service
U.S. Department of Commerce
5285 Port Royal Road
Springfield, VA 22161

13. SUPPLEMENTARY NOTES
NREL Technical Monitor: Lori Greene and Martha Symko-Davies

14. ABSTRACT *(Maximum 200 Words)*
The current work by University of Delaware researchers sought to understand InGaN as the potential material for photovoltaics. Phase separation was identified as a key loss mechanism. Phase-separated material (a lower bandgap) controls the open-circuit voltage, while the non-phase separated material (higher bandgap) controls the absorption. Phase separation in InGaN layers was controlled via optimization of growth conditions and device thickness.

15. SUBJECT TERMS
PV; high efficiency; devices; solar cells; bandgap; open-circuit voltage; ohmic contact; optimization; InGaN; phase separation;

16. SECURITY CLASSIFICATION OF:			17. LIMITATION OF ABSTRACT	18. NUMBER OF PAGES	19a. NAME OF RESPONSIBLE PERSON
a. REPORT	b. ABSTRACT	c. THIS PAGE			
Unclassified	Unclassified	Unclassified	UL		19b. TELEPHONE NUMBER (*Include area code*)

Standard Form 298 (Rev. 8/98)
Prescribed by ANSI Std. Z39.18

F1146-E(09/2007)